Climatic Change (2026) 179:121
https://doi.org/10.1007/s10584-026-04205-5

Air temperature and precipitation trends in the Extended European Alpine Region over 1961–2020 from a dense network of surface weather stations

Giulio Bongiovanni[1,2] · **Anna Napoli**[1,3] · **Michael Matiu**[1] · **Alice Crespi**[4] · **Bruno Majone**[1] · **Dino Zardi**[1]

Received: 3 February 2025 / Accepted: 7 May 2026 / Published online: 20 May 2026

Abstract
The European Alps and their surroundings (hereby referred to as the *Extended European Alpine Region, EEAR*) are known to be a hot-spot of climate change as they are experiencing a faster warming rate than other regions in the world. However, the complex nature of the Alpine terrain makes it more difficult to understand how climatic changes are distributed over space, and in particular with elevation. In this study, we present a comprehensive analysis of how air temperature, precipitation and a broad set of extreme indices have changed over the EEAR during the period 1961–2020, based on a newly developed daily observational dataset with unprecedented spatial density. The analysis relies on robust trend estimation using the non-parametric Sen's slope method, with statistical significance assessed via the Mann–Kendall test. In addition, elevation-dependent climate change is investigated through a twofold approach that accounts for both linear and non-linear patterns. The analysis of the trends of air temperature and precipitation highlights the enhanced warming in the Alpine region, which amounts to about $+2°C$ on average during the 1961–2020 period. In terms of temperature extremes, the same period is characterized by a significant increase in warm spells duration index (WSDI), +10.1 days, and in both minimum and maximum temperature indices, respectively +48 warm nights (TN90p) and +49 warm days (TX90p). While mean precipitation does not show a significant change in time, the frequency of extreme rainfall events (R95p index) significantly increased by about +13 days since 1961. Moreover, an enhanced warming with elevation is observed for mean and minimum temperature from February to May, while increasing precipitation trends with elevation are found, mainly in summer.

Keywords Elevation dependent climate change · European alps · In-situ observations

Extended author information available on the last page of the article

1 Introduction

Recent research results have shown that mountain regions worldwide have been experiencing enhanced warming compared to other regions of the world, making them more vulnerable to climate change (Hock et al. 2019; Cramer et al. 2020). In particular, in the Alpine area and surrounding regions, climate change is already influencing the occurrence and the magnitude of natural hazards, such as floods, heat waves, cold breaks, droughts, landslides and snow avalanches (Beniston 2006; Ménégoz et al. 2020). These phenomena profoundly impact numerous socio-economic and environmental sectors and resources, including tourism, agriculture, hydropower, human health, ecosystems, water, infrastructures, and the mountain cryosphere (Toreti and Desiato 2008; Gobiet et al. 2014; Hock et al. 2019).

However, understanding how the climate is changing in regions of complex orography, such as the European Alps, is a challenging goal, due to the complexity and heterogeneity of the region, coupled with uncertainties in observational data. Limitations of the observational network, scarcity of measurements at high elevations, differences in homogenization methods and mapping procedures are all sources of uncertainty. Despite these limitations, significant progress has been made to improve our understanding of the Alpine climate and its long-term trends. The Alpine climate is shaped by the complex orography of the region and the influence of several climate regimes, such as oceanic, continental, humid subtropical and Mediterranean influenced (Koppen 1936; Beck et al. 2018), resulting in pronounced spatial variability and unique climate features (Beniston 2005).

Climate research in the last two decades has provided increasing evidence of the enhanced warming occurring in the Alpine area compared to surrounding regions (Beniston and Jungo 2002; Moberg and Jones 2005; Toreti and Desiato 2008), highlighting the Alps as a remarkable hot-spot for climate change (Giorgi 2006; Auer et al. 2007; Baettig et al. 2007; Gulev et al. 2021). Indeed, since the late nineteenth century, most of the European Alpine region has been warming twice as fast as the global average of the planet (Auer et al. 2007; Brunetti et al. 2009; Ceppi et al. 2012; Ohmura 2012). However, the warming exhibits different rates depending on different elevations, periods, and regions. Also, the evaluation of trends is strongly affected by the density of the weather stations network considered (Vose et al. 2004; Gulev et al. 2021). In particular, a latitude-dependence of temperature trends across the Alpine range has been observed in recent decades, with a more pronounced warming on the Southern Alps, $+0.49°C$/decade, compared to the northern side, $+0.35°C$ /decade (Pepin et al. 2022). Also, warming trends resulted in more frequent summer days and warm-tropical nights, more persistent heat waves and an overall decreasing occurrence of cold nights and frost days (Moberg and Jones 2005; Toreti and Desiato 2008; Acquaotta et al. 2015).

Precipitation trends over the Alpine region are challenging to detect due to the strong locally-controlled dynamics, significant inter-annual to decadal variability, and spatial variability. In particular, significant trends on time scales shorter than a century are often challenging to capture (Gobiet et al. 2014; Zubler et al. 2014; Rysman et al. 2016; Ménégoz et al. 2020). Despite these challenges, a general decrease in total precipitation over the European Alps has been observed in the last century (Brunetti et al. 2006; Brugnara et al. 2012). Conversely, extreme rainfall events have increased on a continental scale, especially since the 1950s, in both frequency and intensity (van den Besselaar et al. 2013).

Many observational studies show a correlation between warming rates and elevation, although this may vary depending on the season, region and variable (Beniston et al. 1997; Böhm et al. 2001; Rangwala and Miller 2012; Gobiet et al. 2014; Pepin et al. 2015). This phenomenon, known as Elevation Dependent Warming (EDW, Palazzi et al. 2019), is characterized by a systematic difference in warming rates between mountain summits and valleys (Pepin and Lundquist 2008; Pepin et al. 2015). The EDW mechanism is favoured by local effects on the surface energy balance, such as the snow-albedo feedback (i.e., the warming enhancement where the snowline is retreating Pepin and Lundquist (2008)), an increase of specific humidity in initially drier atmospheric conditions (Rangwala et al. 2016), an enhanced radiative forcing change at lower temperatures (Ohmura 2012), decreased aerosol concentrations at higher elevation (Napoli et al. 2019), and clouds. However, EDW remains one of the physical processes occurring in mountainous regions that is not yet fully understood (Pepin et al. 2015, 2022). Despite these uncertainties, the presence of EDW could exacerbate loss of high-altitude cryosphere and changes in mountain ecosystems and precipitation patterns.

In the case of precipitation, a similar phenomenon occurs, commonly referred to as Elevation Dependent Precipitation Change (EDPC, Luce et al. (2013)). However, precipitation variability is even less consistent than temperature variability (Gobiet et al. 2014), and studies focused on EDPC involving observations are very limited. In recent years, the analysis of elevation dependency has been extended to include additional meteorological variables besides temperature and precipitation, and is now commonly referred to as Elevation Dependent Climate Change (EDCC) (Pepin et al. 2022). However, for the European Alps, EDCC has mostly been investigated nationally, based on sparse meteorological networks, and focusing on mean values rather than on extremes (Böhm et al. 2001; Rangwala and Miller 2012).

Here, we present a comprehensive study of air temperature and precipitation changes that occurred in the Alpine region during the period 1961–2020, based on the newly developed EEAR-Clim dataset (Bongiovanni et al. 2025), a high-quality, spatially dense, homogeneous and internally consistent station-based observational product for the Extended European Alpine Region. This research aims to provide a better understanding of the climatology and long-term trends across the European Alps by leveraging the high quality and spatial density of the station network, and by assessing a large set of indices describing extreme conditions. In addition, the elevational coverage of EEAR-Clim is exploited to assess EDCC through a twofold approach that accounts for both linearity and non-linearity of the elevation dependence.

The paper is structured as follows: Sect. 2 frames the study domain from a geographical and climatic perspective, introduces the observational data, and describes the main analysis methods and metrics used; Sect. 3 discusses the main results in terms of trends and analyses elevation dependencies. Sections 4 and 5 report a discussion on Alpine climate changes over 1961–2020 and the main conclusions, respectively.

2 Data and methods

2.1 Study area

The present study focuses on an area encompassing the Extended European Alpine Region (EEAR), shown in Fig. 1, spanning from 3°E to 18°E in longitude and from 43°N to 49°N in latitude. The EEAR domain extends 1100 km East-West and 700 km North-South, covering an area of about 800,000 km^2. The EEAR is centered on the European Alps, but also includes parts of several other sub-alpine mountain ranges, such as the Jura mountains (North-West EEAR, France-Switzerland), the Massif Central (South-West EEAR, central-southern France), the Black Forest (North-West EEAR, south-western Germany), the Bohemian Forest (North-East EEAR, Germany-Czech Republic), the Dinaric Alps (South-East EEAR, Croatia) and the Apennines (South EEAR, central Italy). The EEAR features complex orography with extensive lowlands and deep valleys intersecting both the Alpine and the sub-alpine range and shaping several mountain massifs. Being predominantly a complex terrain region, the EEAR exhibits a strong elevation contrast between the lowlands and the top of the European Alps, 4807 m above sea level (a.s.l.) at the Mont Blanc summit.

The Alps stand out due to their diverse climatic features resulting from the combined influence of North Atlantic weather systems, the Mediterranean Sea, and the large European land mass (Schär et al. 1998; Böhm et al. 2001; Beniston and Jungo 2002; Begert et al. 2005). Moreover, the climate of the EEAR is shaped by the interplay of different regimes, including the influence of oceanic climate in the northern areas, humid subtropical conditions in the southern lowlands, and Mediterranean-influenced climate along the coastal areas. The main Alpine range exhibits colder conditions typical of a continental climate, with sub-arctic and Alpine polar-tundra regimes confined to the highest elevations

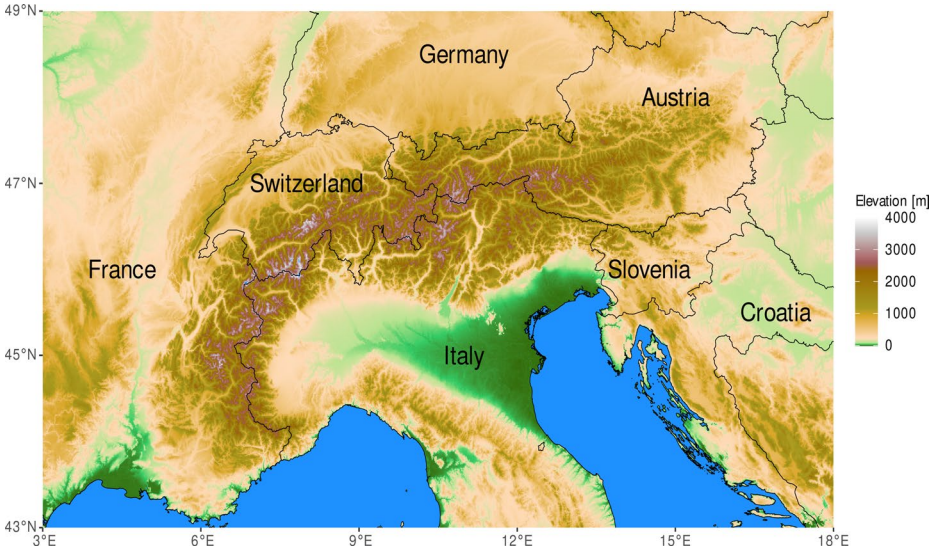

Fig. 1 Overview of the Extended European Alpine region domain. The topography is based on the digital elevation model (DEM) from the shuttle radar topography mission CGIAR-SRTM (90 m resolution) (https://srtm.csi.cgiar.org/). Country borders are retrieved from global administrative areas (GADM) database (https://gadm.org/)

(Koppen 1936; Beck et al. 2018). The complex topography of the region induces local weather phenomena including orographic lifting, air channeling and air blocking, and related effects such as orographic precipitation or rain shadowing. In addition, the region is also prone to thermally-driven orographic phenomena including the Alpine Foehn across the European Alps, the Mistral in the Rhone Valley, the Bora in the north-eastern Adriatic Sea, more local winds such as Ora del Garda over Garda Lake (Italy), or Malojawind in Engadina (Switzerland), as well as thermal inversions in the Po Valley (Auer et al. 2007; Zecchetto et al. 2009; Laiti et al. 2013). The interactions between processes typical of the different climate zones, coupled with the Alpine orography, promote strong spatial and elevational climate gradients (Auer et al. 2007). Moreover, the geography of the Alps and the high mountain range act as a natural barrier, shielding downstream regions against intense Atlantic synoptic perturbations and intercepting moisture-rich Mediterranean inflows, though orographic effects and lee cyclogenesis may enhance precipitation and the severity of weather events in such areas. In addition, the Alpine topography favors the trapping of pollutants and haze, mostly generated by anthropogenic activities in the highly urbanized areas surrounding the Alpine region (Sandrini et al. 2014; Schroeder et al. 2014).

The EEAR extends into the Mediterranean Sea to the South. The Mediterranean area, including southern Europe and northern Africa, has been identified as a climate change hotspot (Gulev et al. 2021), experiencing an amplified warming with strong impacts on several sectors, including cryosphere and hydrological cycle. The proximity of two such hot-spots, the Alps and the Mediterranean region, heightens the vulnerability of the whole area to the impacts of climate change.

2.2 Observational data

The observational data used in this study were extracted from the EEAR-Clim dataset (Bongiovanni et al. 2025), including daily measurements of precipitation (P), mean (T), minimum (Tmin) and maximum (Tmax) air temperature up to 2020. EEAR-Clim dataset is based on time series thoroughly screened applying a comprehensive and deep quality control procedure aimed at assessing internal and temporal consistency, as well as spatial coherence, facing the problem of outliers identification. In addition, time series were tested for data homogeneity by a cross-comparison of break points identified using the Climatol (Guijarro 2023), ACMANT (Domonkos 2015) and RHtests (Wang 2008) methods, and the resulting inhomogeneous periods were adjusted through a quantile matching technique.

We used a subset of the EEAR-Clim dataset (see Fig. 2) that encompasses almost complete time series for the period 1961–2020.Time series were selected based on a trade-off between a minimum period extent of 30 years, homogeneous spatial coverage, and compliance with WMO (2017) requirements in terms of data completeness. Concerning missing observations, a month of data is considered valid if the "5/3" rule is satisfied, i.e. there are no more than five missing daily observations in the whole month and no more than three consecutive missing days (WMO, 1989). A year is deemed valid if there are no more than three missing months (Fioravanti et al. 2019), and these are not consecutive. Finally, time series with at least 80% of valid years over the considered period and no more than four consecutive missing years were selected. The strict criteria adopted allowed for selecting only time series with more than 85% of valid data. Among the selected time series, data completeness exceeded 95% for over 91% of air temperature and 96% of precipitation stations.In total,

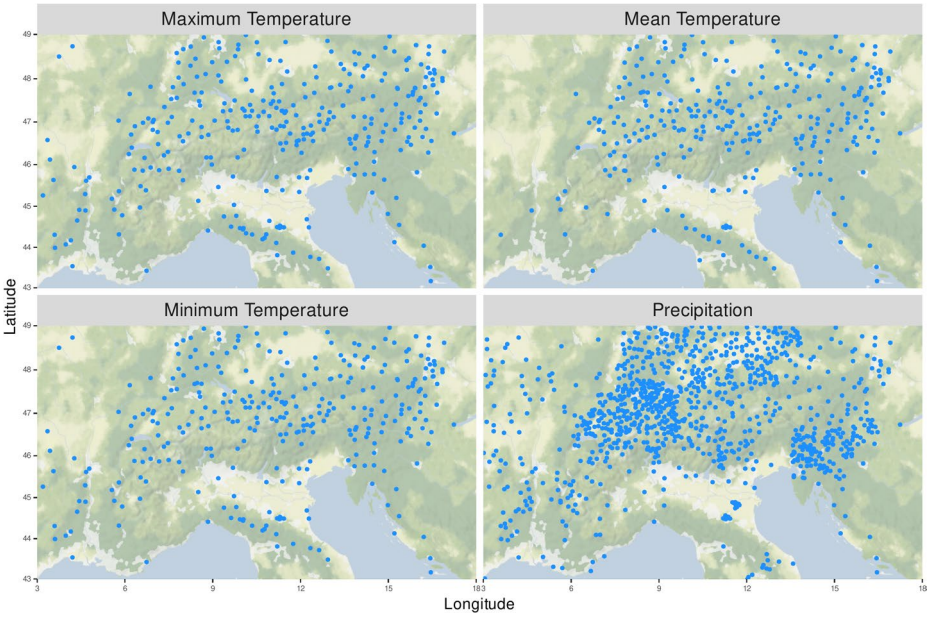

Fig. 2 Distribution of stations selected for the trend analysis, providing daily precipitation (989 time series) and temperatures (mean, minimum and maximum, with respectively 301, 320 and 318 time series) during the 1961–2020 period

the selected subset consists of 301 mean temperature, 320 minimum temperature, 318 maximum temperature, and 989 precipitation time series.

2.3 ETCCDI indices

Several climate indices derived from daily data have been proposed and widely used in the literature to measure and quantify climate variability and trends (Zhang et al. 2011). Most of these indices were developed by the joint Expert Team on Climate Change Detection and Indices (ETCCDI, https://etccdi.pacificclimate.org/), while others are proposed by the European Climate Assessment and Dataset (ECA&D). These indices are designed to monitor, analyze and detect changes in temperature and precipitation extremes at a regional level (Folland et al. 2000; Tank and 2003; Peterson 2005; Toreti and Desiato 2008).

In this work, we considered a subset of 16 indices from the full set provided by ETCCDI and ECA&D, selecting the most suitable for describing changes in the frequency, intensity and duration of temperature and precipitation extremes over the EEAR. An overview of the selected indices is provided in Table 1.

For percentile-based indices (TN10p, TN90p, TX10p, TX90p, R95p, R99p), the percentiles are calculated from the empirical distribution of daily values observed during the period 1961–1990, following ETCCDI recommendations, using the function $ts2clm$ from the R package $heatwaveR$ (Schlegel and Smit 2021). This methodology allows for a consistent

Table 1 Overview of air temperature (T) and precipitation (P) extreme indices analyzed in this study. The acronym, the extended name and the definition are reported below. Indices definition based on ECA&D classification is highlighted as an asterisk

Index	Description	Definition
GSL	Growing season length	Count of days between first spans of at least 6 days with $T > 5°C$ and, after July 1st, with $T < 5°C$
TR	Tropical nights	Count of days when $Tmin > 20°C$
SU	Summer days	Count of days when $Tmax > 25°C$
FD	Frost days	Count of days when $Tmin < 0°C$
ID	Icing days	Count of days when $Tmax < 0°C$
WSDI	Warm spell duration index	Count of days with at least 6 consecutive days when $Tmax > 90^{th} percentile$
CSDI	Cold spell duration index	Count of days with at least 6 consecutive days when $Tmin < 10^{th} percentile$
TN10p	Cold nights	Percentage of days when $Tmin < 10^{th} percentile$
TX10p	Cold days	Percentage of days when $Tmax < 10^{th} percentile$
TN90p	Warm nights	Percentage of days when $Tmin > 90^{th} percentile$
TX90p	Warm days	Percentage of days when $Tmax > 90^{th} percentile$
R20mm	Very heavy precipitation days	Count of days when $P \geq 20mm$
R95p*	Very wet days	Percentage of days when $P \geq 1mm$ and $P > 95^{th} percentile$
R99p*	Extremely wet days	Percentage of days when $P \geq 1mm$ and $P > 99^{th} percentile$
CDD	Duration of dry spells	Maximum number of consecutive days when $P < 1mm$
CWD	Duration of wet spells	Maximum number of consecutive days when $P \geq 1mm$

baseline to evaluate changes in the frequency of extreme events over time and compare the findings among different regions and studies. These indices are computed annually, but seasonal estimates are also provided in the Supplementary Material. Spell-related (WSDI, CSDI, CDD, CWD) and temperature percentile-based (TN10p, TN90p, TX10p, TX90p) indices are computed on a 5-day moving window, following the ETCCDI definition.

2.4 Trend analysis

The analysis of trends aims to study the evolution of temperature, precipitation, and extreme indices in the EEAR during the 1961–2020 period. Daily time series of precipitation, as well as minimum, maximum and mean temperatures, were averaged for temperature and accumulated for precipitation values to monthly, seasonal, and annual time scales. This aggregation procedure does not apply to extreme indices, which are computed annually and seasonally based on the raw daily time series. Trend analysis was performed both on single-station and on spatially-averaged time series using the non-parametric Theil-Sen estimator (Sen 1968), a robust regression technique based on the median of pairwise slopes that is commonly applied in climate research. Trends were estimated using single-station time series and

Note that units of trends in extremes are made uniform by converting TN10p, TN90p, TX10p, TX90p, R95p and R99p from *percentage of days/decade* to *days/decade* by multiplying values by 3.65 (i.e. 365 days divided by 100).

The statistical significance of trends is assessed through the Mann-Kendall non-parametric test (Sneyers 1990) at 99 ($p < 0.01$) and 95 ($p < 0.05$) confidence levels.

2.5 Analysis of elevation-dependency

The study of elevation-dependency aims to assess EDW and EDPC patterns over the EEAR. Trends computed for each station are aggregated into 20 partly overlapping elevation classes (see below), each including approximately the same number of stations to reduce the variability due to the different sizes of the sample in each elevation range, as other elevation-dependent studies proposed Napoli et al. (2023). The elevation intervals were then adjusted to be consistent across all variables and to include at least 30 and 70 stations per class, respectively, for air temperature and precipitation, and to have the same classes for all variables. The final 20 bands have the following ranges: 0–155, 65–200, 165–260, 210–300, 275–350, 315–415, 375–455, 430–485, 465–535, 490–575, 555–640, 585–720, 665–835, 745–950, 865–1070, 985–1255, 1090–1435, 1315–1805, 1510–2515, and 1595–3600 m.

To evaluate the magnitude and uncertainty of trends in each elevation band, we computed the median and the median absolute deviation (MAD), respectively. These indexes were adopted for their robustness and insensitivity to outliers (Leys et al. 2013; Hunziker et al. 2018) as compared to the mean and standard deviation. However, estimates based on mean and standard deviation are also computed and reported for comparison purposes only.

The linear rate of the EDCC signal was estimated by regressing the median trend of each elevation band against the midpoint elevation of the corresponding band using the robust Theil-Sen method. The statistical significance was assessed using the Mann-Kendall test at the 95% and 99%. Recognizing that trend-elevation dependency, if occurring, can also be non-linear, we additionally interpolated the median trends with the LOcal regrESSion

(LOESS, sometimes also called Savitzky–Golay filter) method to capture possible departures from linearity (Palazzi et al. 2019). In the case of extremes, only a selection of all the percentile-based indices (TN10p, TX10p, TN90p, TX90p, WSDI, CSDI, R95p, and R99p) was used to study their elevation patterns.

The analysis of the elevation-dependency was completed by assessing how fixed-threshold temperature indices (CDD, CWD, FD, ID, R20mm, GSL, SU, TR) changed in the elevation range where they occurred. We compared the change in both minimum and maximum elevation from 1961 to 2020, and then evaluated the statistical significance of the observed changes, at 95% confidence level, by applying the Mann-Kendall test to the annual elevation time series.

3 Results

3.1 Trends in mean values

Air temperature time series show a clear evolution towards warming conditions at both annual and seasonal scales (Fig. 3) over 1961–2020, with the strongest trends in spring (MAM) and summer (JJA). Time series also highlight the record value reached in summer 2003 when a severe heatwave occurred (Garcia-Herrera et al. 2010), which is seen in

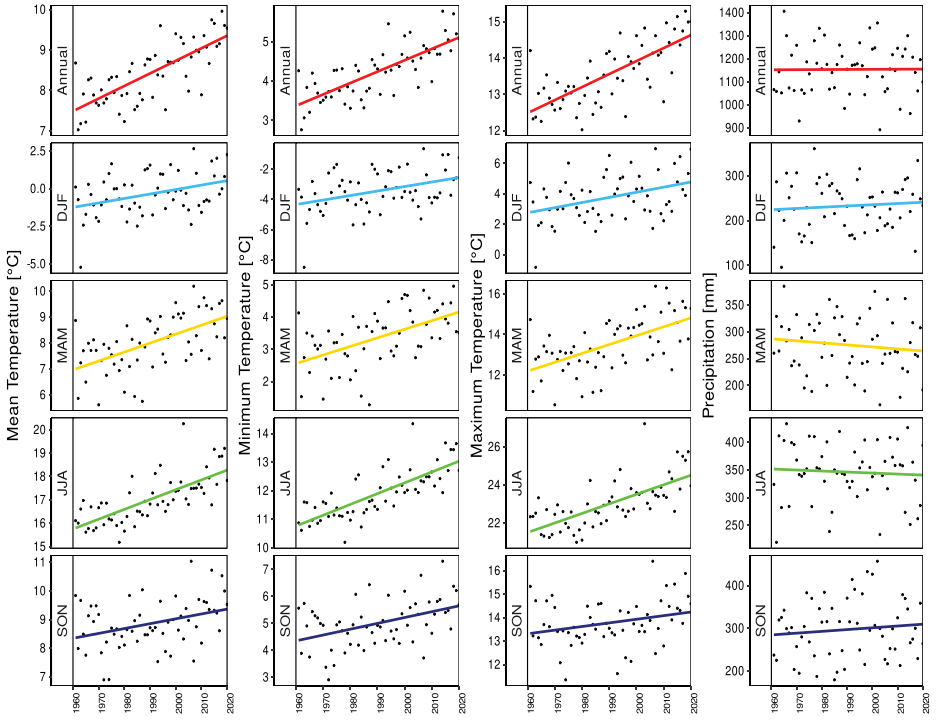

Fig. 3 Time series of annual and seasonal values of precipitation and mean, minimum and maximum temperature averaged over the Alpine region for the period 1961–2020. Straight lines show the linear fit. R^2 values are provided in Table S2

the JJA panels of temperature (Fig. 3). Conversely, the coldest conditions are bound to the beginning of the time series, with the lowest temperatures recorded in winter 1962/1963 (DJF panel in Fig. 3).

Stronger and statistically significant ($p < 0.01$) trends (Table 2) are found from mid-spring (April) to late Summer (August) for 96.2% of stations, with the maximum warming rates in August: $0.4°C$, $0.48°C$ and $0.58°C$/decade for Tmin, T and Tmax, respectively. Winter (DJF) and autumn (SON) temperature trends show more variability than other seasons. Weaker, but still significant trends ($p < 0.05$, 63% of stations) are found from November to January. The strongest trends across winter and autumn months are observed in December, particularly for Tmin, which is experiencing the highest increase ($0.4°C$/decade). The probability density function (PDF) of monthly trends (Fig. S1) shows a clear difference between the summer months, with intensified warming conditions, and the early-mid autumn, when trends are the lowest. On an annual scale, air temperature increased at an average rate of $0.32°C$ per decade, leading to a warming of about $+2°C$ since the 1960s. However, the spatial distribution of trends (Fig. S2) highlights an uneven warming across the EEAR, with more pronounced warming over the southern and north-eastern parts of the Alpine region. Our results also show a lower trend for annual minimum temperature compared to the annual maximum temperature, +0.29 and $+0.39°C$ per decade, respectively.

Precipitation time series exhibit larger variability and consequently have mostly non-significant trends ($p > 0.05$) compared to air temperature for about 90% of stations. However, the spatial distribution of trends (Fig. S2) shows increasing precipitation observed across the northern Alps, where wetter conditions generally prevail, while decreasing precipitation totals are observed mostly over the southernmost side of the region and in Slovenia.

3.2 Trends in extremes indices

All temperature-related indices exhibit strong and significant trends (Table 2 and Fig. 4), supporting the results obtained for annual and seasonal temperatures. The robustness of such rates is supported by the number of stations with statistically significant ($p < 0.05$) trends, of about 93% or higher for most indices, with lower percentages (70%) for cold extremes (FD, ID, CSDI).Since 1961, SU has increased at a rate of 4 days per decade, TN90p and TX90p exhibit an increase of more than 8 days per decade, while a trend of +0.7 days per decade is found in the case of TR. These warming trends are also reflected in decreasing trends for cold extreme indices, with TN10p and TX10p declining at a rate of −4 days per decade and FD at a rate of −3 days per decade.

Warming conditions found in trends of extreme temperature indices are increasingly persistent, with increased duration of warm spells (WSDI) and reduced duration for cold spells (CSDI). The warming climate is also associated with an increased length of the meteorological growing season for vegetation, quantified at about +4 days per decade.

At the seasonal scale, percentile-based temperature indices (TN10p, TX10p, and TN90p) show similar results to seasonal averages (Table S3). TX90p shows the highest trend values between spring and summer, the same period when air temperature trends are stronger and more significant.

Precipitation extremes show significant positive trends (30% of stations), leading to more frequent intense rainfall events, with change rates of +1.64 and +1.22 days per decade for R95p and R99p indices, respectively. Only dry and wet spells duration indices show no

Table 2 Summary table of regional trends. The left part of the table shows trends of precipitation (P) and mean (T), minimum (TMIN) and maximum (TMAX) temperature at annual, seasonal and monthly time scales, while the right part shows the trends of annual extreme indices. Trends in extremes are made uniform by converting percentile-based indices (TN10p, Tn90p, TX10p, TX90p, R95p and R99p) from *percentage of days/decade* to *days/decade*, multiplying them by 3.65. Different levels of confidence are used: 99% (**) and 95% (*)

PERIOD	T[°C/10yr]	TMIN[°C/10yr]	TMAX[°C/10yr]	P [mm/10 yr]	INDEX	TREND [Days/10 yr]
Annual	0.32**	0.29**	0.39**	0.2	**GSL**	4.11**
DJF	0.27*	0.24*	0.30**	1.7	**SU**	4.14**
MAM	0.34**	0.27**	0.44**	−1.6	**TR**	0.71**
JJA	0.41**	0.36**	0.48**	−0.5	**FD**	−3.20**
SON	0.18*	0.21**	0.16*	1.5	**ID**	−1.94**
Jan	0.32*	0.33*	0.36*	0.7	**TN10p**	−4.45**
Feb	0.20	0.16	0.30	−0.2	**TN90p**	8.03**
Mar	0.34*	0.27*	0.45*	−3.4	**TX10p**	−4.20**
Apr	0.40**	0.28**	0.50**	−3.7*	**TX90p**	8.21**
May	0.36**	0.29**	0.42**	0.3	**WSDI**	1.68**
Jun	0.41**	0.38**	0.50**	−1.7	**CSDI**	−0.35**
Jul	0.41**	0.36**	0.50**	0.3	**R20mm**	0.42**
Aug	0.48**	0.40**	0.58**	−1.2	**R95p**	1.64**
Sep	0.09	0.12	0.10	7.1	**R99p**	1.22**
Oct	0.16	0.24*	0.09	4.8	**CDD**	−0.23
Nov	0.27*	0.30**	0.27*	−2.2	CWD	−0.15
Dec	0.36**	0.40**	0.37**	2.4		

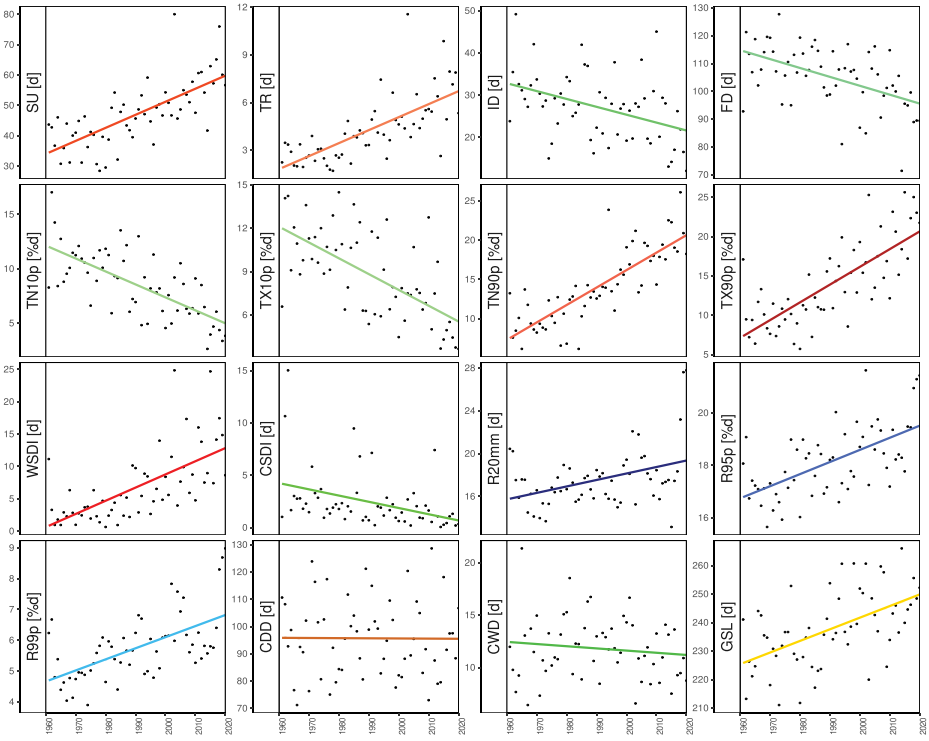

Fig. 4 Time series of annual values of 16 selected extremes indices averaged over the Alpine region for the period 1961–2020. Straight lines show the linear fit. R^2 values are provided in Table S2

significant trends, mainly due to strong variability in the values. At the seasonal scale (Table S3), extreme rainfall days (R95p and R99p) show stronger trends in winter and spring than in summer and autumn, while remaining positive and highly significant in all seasons except for R95p in autumn.

3.3 Elevation-dependency of trends

Linear EDW rates (Table 3) differ between seasons and temperature variables. Negative elevation-dependency for air temperature trends is observed from early autumn to mid-winter, with maximum rates for T in October ($-0.085°C decade^{-1} km^{-1}$) and Tmax in January ($-0.138°C decade^{-1} km^{-1}$). From late winter (February) to late spring (May) we observed a positive EDW for T and Tmin, with the latter showing its maximum rate of $+0.134°C decade^{-1} km^{-1}$ in April. Tmax does not exhibit significant positive rates, maintaining a negative EDW for most of the year with negligible rates from April to June. In July, a significant and negative trend-elevation linear dependency is observed for T and Tmax ($-0.05°C decade^{-1} km^{-1}$).

However, the linear estimation of EDW rates might mask some non-linearities, as revealed by the elevation distribution of trends at annual and seasonal scales. As shown in Fig. 5, mean, maximum, and minimum temperature trends exhibit different elevation patterns depending on the season. Below 1000 m, trends of mean and maximum temperature

Table 3 Summary table of EDCC linear rates computed over 1961–2020. EDCC is commonly measured in$^{\circ}C\,km^{-1}decade^{-1}$or mm$km^{-1}\,decade^{-1}$equivalent to a change in temperature lapse rate and precipitation-elevation changes over time. Left part of the table shows rates of precipitation (P) and mean (T), minimum (TMIN) and maximum (TMAX) temperature change at annual, seasonal and monthly time scales. The right part shows rates of change in annual extreme indices. Statistical significance is represented by **($p < 0.01$) and *($p < 0.05$). Significant positive and negative rates are highlighted in orange and green, respectively

PERIOD	T	TMIN	TMAX	P	INDEX	TREND
	$\left[\frac{^{\circ}C}{10yr*km}\right]$	$\left[\frac{^{\circ}C}{10yr*km}\right]$	$\left[\frac{^{\circ}C}{10yr*km}\right]$	$\left[\frac{mm}{10yr*km}\right]$		$\left[\frac{Days}{10yr*km}\right]$
Annual	−0.019	0.025*	−0.058**	0.59**	**TN10p**	0.059
DJF	−0.045**	−0.012	−0.099**	−0.56	**TX10p**	0.148**
MAM	0.022**	0.072**	−0.037*	−0.09	**TN90p**	0.125
JJA	−0.013	0.023	−0.023*	1.80**	**TX90p**	−0.296**
SON	−0.031**	−0.035**	−0.049**	0.51*	**R95p**	−0.047
Jan	−0.081**	−0.068**	−0.138**	0.99	**R99p**	0.013
Feb	0.014	0.058**	−0.060**	−1.32**	**WSDI**	−0.229*
Mar	0.001	0.053**	−0.077**	−0.57	**CSDI**	−0.053**
Apr	0.063**	0.134**	0.013	0.32		
May	0.021	0.043*	0.004	−0.22		
Jun	0.012	0.039*	0.004	2.06**		
Jul	−0.051**	0.008	−0.052**	−0.02		
Aug	−0.019	0.046*	−0.022	2.79**		
Sep	−0.048**	−0.039*	−0.060**	−0.30		
Oct	−0.085**	−0.086**	−0.042**	0.39		
Nov	−0.003	0.014	−0.024	−0.69		
Dec	−0.052**	−0.019	−0.130**	0.46		

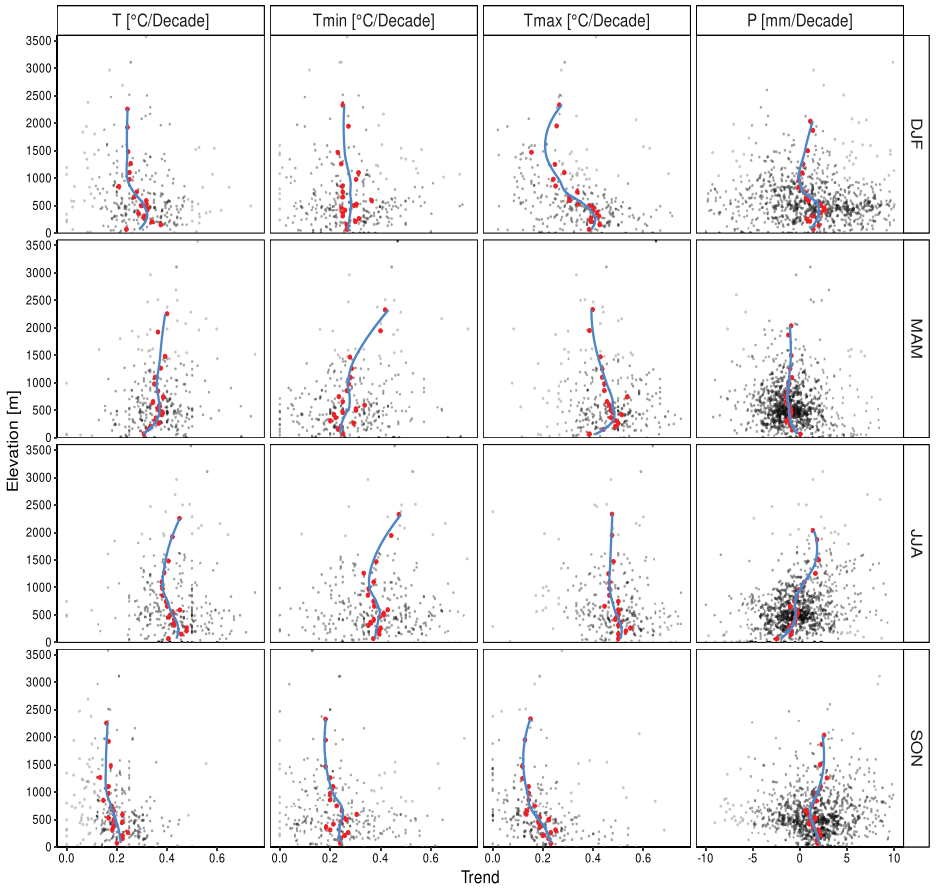

Fig. 5 Distribution of seasonal trends with elevation for precipitation (P) and mean (T), minimum (Tmin), and maximum (Tmax) temperature. Median trend in each elevation band (red points), and the related interpolating line (in blue), are shown together with station trends (black points). Median points values and uncertainties are reported in Tables S4 and S5

increase with elevation up to 500 m, while the magnitude of trends decreases with elevation in the 500–1000 m band. Minimum temperature trends do not show clear changes with elevation up to 1000 m. In addition, no elevation patterns are found for T, during autumn, and Tmax, in summer. Above 1000 m, Tmin and T trends generally increase with elevation, especially on an annual scale, in summer, and, for Tmin only, in spring. Tmax trends are mainly characterized by a strong variability with elevation and across the seasons.

For precipitation, a positive EDPC is observed mainly in summer, with significant rates in June and August, and in the autumn season (Table 3). Annually and in SON, significant EDPC rates show a clear increase only between 1000 and 1500 m. During winter, the pattern of precipitation trends with the elevation is characterized by an alternating shape: higher precipitation trends are observed between 500 and 1000 m, and lower otherwise. However, precipitation trends show markedly higher uncertainties (Table S4). In particular, evaluating the relative uncertainties as a percentage of the median trends, they are typically at least ten times larger than those observed for air temperature trends (Table S4 and S5). This

discrepancy is even more pronounced when using mean and standard deviation (Table S6), more sensitive to statistical outliers, further supporting the choice of median-based metrics as more robust estimators.

The analysis of EDW and EDPC patterns is extended to trends of eight selected extreme indices (Fig. S4). Negative trends are observed for cold days (TX10p) and cold nights (TN10p) at all elevations, but with a less negative tendency in the 500–1500 m range. In particular, TX10p trends in this elevation range show a significant positive rate of 0.148% of $daysdecade^{-1}km^{-1}$, meaning a stronger decrease of cold days at lowlands compared to higher elevation. Conversely, higher trends of warm nights (TN90p) above 1000 m align with Tmin behavior. Trends in warm days (TX90p) exhibit a significant decrease with elevation (−0.296% $daysdecade^{-1}km^{-1}$) with lowlands, up to 500 m, experiencing a stronger increase of warm days compared to high elevations. A similar negative pattern with elevation in the 0–500 m range is observed for the warm spell duration (WSDI), in contrast to the enhanced warming of air temperature at the lowest elevations. Contrarily, CSDI trends, which report an overall significant relation with elevation of −0.053% $daysdecade^{-1}km^{-1}$, decrease with elevation in the 0–500 m range and increase in the 800–1500 m range, partially aligning with the elevation pattern of Tmin trends. The trends in precipitation extremes show no significant elevation pattern, with small EDPC rates, particularly for the R95p index. The absence of EDPC for very extreme rainfall (R99p) is influenced by a reduction in trends in lowlands and an increase at higher elevations, more pronounced above 1500 m (Fig. S4).

As some temperature indices depend on a fixed threshold (e.g., ID on $0°C$, SU on $25°C$), and temperature strongly depends on elevation, we assessed changes in the elevation range where thresholds of these indices are reached (Table S8). The ID index exhibited a small increase in the minimum elevation where Tmax remains below $0°C$. GSL, SU and TR indices showed a statistically significant ($p < 0.05$) increase in the maximum elevation where the temperature reaches the related fixed thresholds. In particular, the maximum elevation increased by 880 m for GSL, from 2691 m to 3571 m, by 453 m for SU, reaching 2063 m in 2020, while TR reached up to 1979 m in 2020 with an increase of 911 m in 60 years.

4 Discussion

The comprehensive analysis of 1961–2020 average climate conditions, long-term trends and their elevation dependency in the Extended European Alpine Region (EEAR), based on a spatially dense dataset of quality-checked and homogenized time series of air temperature and precipitation, provides a broad and detailed overview of the climate changes affecting this complex region.

The choice of the subset of stations used for the analysis relies on rigorous criteria, allowing for the selection of time series with a high percentage of valid data, while preserving the homogeneity of the spatial distribution of the stations. A sensitivity analysis estimating the trend magnitude after excluding time series with completeness below 95% (Table S1), showed no variations or significant changes compared to the rates estimated using the whole subset. These findings support the validity of rules applied to select time series and the robustness of the estimated trends.

Since 1961, there has been a significant increase in air temperature in the European Alps, estimated at about $+2°C$, at both annual and seasonal scales, with higher rates mostly during spring and summer. Thus, temperature values comparable to those experienced during the memorable summer of 2003, and even higher, are likely to be measured in the future, following the estimated trends and observations during the most recent years (2017–2020). Conversely, conditions characterized by strong negative anomalies are unlikely to repeat in the next centuries as a consequence of global warming, albeit still physically possible (Sippel et al. 2024). The estimated warming rates are consistent with previous analyses (Auer et al. 2007; Brunetti et al. 2009; Ceppi et al. 2012; Rottler et al. 2019), though we found higher trends in winter. However, winter season, and also autumn, showed the largest spatial variability in temperature trends across stations, likely due to the influence of changes in snow cover and albedo, as well as the increased variability of atmospheric circulation patterns, mostly during winter months (Beniston et al. 1997).

The Tmin-Tmax asymmetry observed predominantly in November and December, with Tmin trends higher than Tmax, aligns with the scientific literature (Böhm et al. 2001; Beniston 2006; EEA, 2009). This suggests that a faster increase of minimum temperatures may contribute to the observed reduction of snow cover during winter months (Gobiet et al. 2014), by delaying the onset of the snow season (Hock et al. 2019). However, studies focused on more recent periods at the global and European levels showed a reversed behavior with a stronger increase of maximum than minimum temperature (Curci et al. 2021), in line with our findings for the rest of the year. We can observe that the discrepancy between trends of Tmin and Tmax increases as they approach their maximum trend values, in April and during summer, suggesting a disproportional daytime warming that may have dramatic implications for society, especially if this tendency continues in the next decades. The enhanced diurnal cycle may be explained by soil drying during summer, a springtime modulation of the snow-albedo feedback linked to the evolution of snow cover extent and distribution, and the influence of circulation patterns and associated meteorological conditions to favor an amplified daytime radiative forcing.

The significant warming also involves extreme high temperatures, which are becoming more frequent, with increasingly persistent conditions, primarily attributable to summertime when higher warming trends are found. However, both cold and warm indices show statistically significant but diverging rates, with negative trends for the former (e.g. TN10p) and positive trends for the latter (e.g. TN90p), that reflect the shift towards higher values in the annual temperature distribution under warming conditions. These strong and robust rates could be explained by the natural variability amplified by anthropogenic warming (Stocker et al. 2013), as well as the influence of soil moisture (Mueller and Seneviratne 2012), warming enhancement related to the snow-albedo feedback (Pepin and Lundquist 2008), radiative forcing effects (Ohmura 2012), and changes in aerosol concentrations (Napoli et al. 2019). The warming climate also influences the vegetation, with an increased length of meteorological growing season favoring anticipated leaf unfolding and delayed leaf coloring. This is consistent to observations of several studies, highlighting plant phenology as one of the more reliable bioclimatic indicators of climate change (Piao et al. 2019; Menzel et al. 2020; Inouye 2022).

The assessment of precipitation trends is more complex due to the high uncertainty in estimated rates, and being not statistically significant for most of the stations. This is likely related to the greater temporal and spatial variability of precipitation especially when time

series shorter than a century are considered (Schmidli et al. 2002; Gobiet et al. 2014; Ménégoz et al. 2020). Conversely, statistically significant increases of heavy rainfall events are not limited to summer (Panziera et al. 2018; Dallan et al. 2022), but are observed in all seasons, aligning to (Ménégoz et al. 2020). This, in combination to the strong warming and the increased persistency of extreme temperatures, may further enhance the sensitivity and vulnerability of the European Alps to the ongoing climate change throughout the year. Accordingly, attention should be paid not only to the summer, but also to other seasons.

The spatial distribution of trends highlights an uneven warming over the EEAR. For instance, warming is more pronounced over the southern and north-eastern sides of the Alpine region, consistent with findings of several studies (Beniston 2006; Auer et al. 2007; Gobiet et al. 2014; Pepin et al. 2022). In contrast, precipitation exhibits diverging patterns across the main Alpine ridge, with wetter conditions over the northern Alps compared to the southern side and Slovenia, in agreement with other assessments (Brunetti et al. 2009, de Luis et al. 2014; Gobiet et al. 2014; Kotlarski et al. 2023; Monteiro and Morin 2023). However, spatial patterns of climate change are more robustly identified through regionalization approaches (Auer et al. 2007) by assessing trends at sub-regional scale, which is beyond the scope of the present study.

The elevation-dependency of air temperature trends shows a higher degree of agreement with model-based studies, as compared to other assessments based on in-situ observations. This is mainly due to the larger number of stations involved in this study and the better coverage of the whole elevation range. However, the agreement with model-based studies is limited to seasons when an enhanced warming with elevation is detected, such as from late winter (February) to late spring (May), and to climate projections including a strong snow-albedo feedback (Palazzi et al. 2019; Pepin et al. 2022; Napoli et al. 2023; Ferguglia et al. 2024). This suggests that a decreasing snow-albedo effect related to reducing snow-ice coverage may act as a key mechanism explaining the enhanced warming at higher elevations and in spring season (Pepin and Lundquist 2008; Pepin et al. 2015; Palazzi et al. 2019). The negative EDW found in our study from early autumn to mid-winter disagrees with model results, while our findings align better to other observational studies focusing on parts of the alpine range (e.g. Tudoroiu et al. 2016). While this disagreement might be due to the different nature of observations and climate models, is it also important to understand whether this involves all the European Alps or is a more local pattern.Reductions in atmospheric aerosol loadings, mostly at lower elevations, contribute to enhancing the global radiation brightening combined with the greenhouse warming, thereby favoring the negative elevation-dependent warming, particularly during autumn and winter. Instead, the negative EDW observed for Tmax in summer suggests additional mechanisms at play, such as changes in cloud cover, enhanced convective activity, land-use and land-cover changes, and water vapour feedback (Giorgi et al. 1997; Pepin and Lundquist 2008; Rangwala and Miller 2012; Philipona 2013; Tudoroiu et al. 2016).

The assessment of EDPC patterns is more complex (Gobiet et al. 2014; Pepin et al. 2022; Napoli et al. 2023; Ferguglia et al. 2024), likely due to the higher intrinsic variability of precipitation. However, a significant positive elevation-dependency was shown in summer, aligning with previous studies (Ferguglia et al. 2024). This could be attributed to a larger drying at the lowest elevations, but also to a more pronounced increase of precipitation at higher elevations.

The increase of precipitation at higher elevations is also supported by an increasing tendency of very heavy rainfall above 1500 m, although the elevation dependency is rather non-linear. Instead, the resulting drier conditions in lowlands are favored by the stronger trends at mid-low elevations in temperature extremes, which reflect the amplification of warming resulting from longer heatwaves and higher winter temperatures, and contribute to snow-to-rain shift or reduction in total precipitation. However, the elevation at which extreme conditions (e.g. summer days or tropical nights) occur is progressively rising to over 2000 m, favoring the reduction of the mountain cryosphere and the increase of slope instability (Beniston 2006; Gobiet et al. 2014; Ménégoz et al. 2020). Moreover, more frequent extreme conditions in higher elevations, associated with shorter and delayed snow seasons, may dramatically affect the water availability in downstream regions, with deep implications for agriculture, hydropower production, human health, industry, wildfire and hydro-geological risk management (Gobiet et al. 2014; Hock et al. 2019, van; Hamel and Brunner 2024; Cornale et al. 2025; Gerberding and Schirpke 2025).

The robustness of EDCC rates was enhanced by adopting overlapping elevation bands of variable width, each one including the same number of stations. This has the advantage of smoothing out the higher uncertainty in upper elevations, keeping it constant across the profile, while preserving the detail at higher elevations. Despite the larger number of high-elevation time series used in this study, the distribution of stations across elevation still results in elevations bands that are denser at lower elevations and wider above 2000 m. This is mainly due to the fact that measurements in high-mountain stations only recently started, with only 8.5% of available time series covering the period 1961–2020, while they increase to 21% for 1991–2000 and to 60% after 2000s. Thus, the study of the station-based EDCC signal considering shorter and more recent periods (e.g. 1995–2025 or 2001–2030), may enhance the accuracy of elevation patterns, in particular above 2000 m. Moreover, the elevation-dependency of trends was found to be non-linear for most of variables and seasons, so non-parametric methods or approaches specifically designed for non-monotonic signals may reveal more complex patterns and better capture the "nose-structure" of EDCC profiles, which is missed using linear regression methods.

5 Conclusions

This work provides an extensive study of the main climate features in the Extended European Alpine Region (EEAR) from 1961 to 2020, based on the analysis of a set of selected indexes evaluated on a dense and homogenized database of temperature and precipitation time series.

Drawing conclusions on the climate features exhibited by EEAR, the following take-home messages can be highlighted:

- The EEAR has experienced a significant average warming of about $2°C$ across 1961–2020, more pronounced from mid-spring to late summer and in early winter, with an acceleration since the early 1990s.
- The overall warming is amplified in air temperature extremes, resulting in more persistent and frequent high-temperature conditions and in a reduction of cold extremes as a result of warmer winters.

- While average precipitation does not show any clear trend, a significant increase in the frequency of heavy rainfall events was identified over the 60 years analyzed.
- The assessment of the elevation dependency of trends reveals the presence of Elevation Dependent Climate Change with:
  - A well-defined positive elevation dependency of temperature from late winter to late spring
  - A negative EDW signal from early autumn to mid-winter and, limited to Tmax, during summer
  - A robust positive EDPC, mainly in summer, along with an increase in extreme rainfall events at higher elevations.
- Additionally, extreme temperatures are occurring at increasingly higher elevations, indicating that this pattern is likely to persist into the future and affect an even larger area of the EEAR.

These findings emphasize how the natural variability, such as the complex precipitation-orography interplay and feedback mechanisms, especially regarding the seasonal snow-albedo effect on temperature trends, plays key roles in shaping regional climatic changes. The progressive extent of extreme warm events to even higher elevations is expected to give rise to significant changes in the Alpine environment, with dramatic consequences in mountain ecosystems and downstream regions.

The approach adopted in this work can be readily applied to other areas or time periods and extended to other climate variables. For instance, a study of trends and their elevation dependency for other essential climate variables is needed to better understand the seasonal variability, the climate drivers of elevation patterns, the distribution of moisture availability at different elevations, and assess the potential impacts, e.g., on renewable energy potential in Alpine areas. Extreme indices also need more extensive studies, especially for their elevation patterns, given their key role in providing a better understanding of climate change impacts on the mountain environment. In this context, assessing how trends are spatially distributed is essential to highlight local differences in the observed patterns and to identify potential areas that are more vulnerable and sensitive to the ongoing climate changes.

The analyses provided in this study and the forthcoming applications would also offer a robust tool for better understanding climate change patterns, drivers and dynamics in the European Alps, improving the reliability of model simulations and future scenarios, and being the basis for more comprehensive studies that integrate model simulations with observational data. All these approaches would provide a robust foundation for targeted adaptation and mitigation strategies, in particular for regions that are highly vulnerable and sensitive to ongoing climate changes.

Supplementary Information The online version contains supplementary material available at https://doi.org/10.1007/s10584-026-04205-5.

Acknowledgements This paper and related research have been conducted during and with the support of the Italian national inter-university PhD School on Sustainable Development and Climate change (http://www.phd-sdc.it). Anna Napoli has been supported by "Fondazione CARITRO" (Cassa di Risparmio di Trento e Rovereto) which is also acknowledged. Bruno Majone and Dino Zardi also acknowledge support from "iNEST (Interconnected Nord-Est Innovation Ecosystem)" project funded by the European Union under

NextGenerationEU (PNRR, Mission 4.2, Investment 1.5, Project ID: ECS 00000043). Michael Matiu and Bruno Majone acknowledge funding from the European Union - NextGenerationEU, PRIN 2022 PNRR (Prot. no. P20227NPLW, CUP E53D23021860001).

Author contributions The original idea of the work was conceived by Giulio Bongiovanni, Dino Zardi and Bruno Majone with the help of the other co-authors. The methodology was elaborated by Giulio Bongiovanni with the help of all co-authors. The analysis of results was performed by Giulio Bongiovanni. The first draft of the paper was prepared by Giulio Bongiovanni with the help of Anna Napoli. All co-authors contributed to reviewing, revising and refining the manuscript.

Funding Open access funding provided by Università degli Studi di Trento within the CRUI-CARE Agreement.

Data availability No new data were generated. Source of analyzed data can be found in the methods description (https://doi.org/10.5281/zenodo.10951609, Bongiovanni et al. 2024).

Code availability All code used in the analysis is available upon request to the corresponding author.

Declarations

Ethics approval Not applicable.

Consent to participate Not applicable.

Consent for publication Not applicable.

Conflict of interest The contact author has declared that none of the authors has any competing interests.

References

Acquaotta F, Fratianni S, Garzena D (2015) Temperature changes in the north-western Italian alps from 1961 to 2010. Theor Appl Climatol 122(3–4):619–634. https://doi.org/10.1007/s00704-014-1316-7

Auer I, Böhm R, Jurkovic A, Lipa W, Orlik A, Potzmann R, Schöner W, Ungersböck M, Matulla C, Briffa K, Jones P, Efthymiadis D, Brunetti M, Nanni T, Maugeri M, Mercalli L, Mestre O, Moisselin J-M, Begert M, Müller-Westermeier G, Kveton V, Bochnicek O, Stastny P, Lapin M, Szalai S, Szentimrey T, Cegnar T, Dolinar M, Gajic-Capka M, Zaninovic K, Majstorovic Z, Nieplova E (2007) Histalp—historical instrumental climatological surface time series of the greater alpine region. Intl J Climatol 27(1):17–46. https://doi.org/10.1002/joc.1377

Baettig MB, Wild M, Imboden, Imboden DM (2007) A climate change index: where climate change may be most prominent in the 21st century. Geophys Res Lett 34(1). https://doi.org/10.1029/2006GL028159

Beck HE, Zimmermann NE, McVicar TR, Vergopolan N, Berg A, Wood, Wood EF (2018) Present and future köppen-geiger climate classification maps at 1-km resolution. Sci DataSci Data 5, 180214 (1). https://doi.org/10.1038/sdata.2018.214

Begert M, Schlegel T, Kirchhofer W (2005) Homogeneous temperature and precipitation series of Switzerland from 1864 to 2000. Intl J Climatol 25(1):65–80. https://doi.org/10.1002/joc.1118

Beniston M (2005) Mountain climates and climatic change: an overview of processes focusing on the European alps. Pure Appl Geophys 162(8–9):1587–1606. https://doi.org/10.1007/s00024-005-2684-9
Beniston M (2006) Mountain weather and climate: a general overview and a focus on climatic change in the alps. Hydrobiologia 562(1):3–16. https://doi.org/10.1007/s10750-005-1802-0
Beniston M, Diaz H, Bradley R (1997) Climatic change at high elevation sites: an overview. Climatic Change 36(3–4):233–251. https://doi.org/10.1023/A:1005380714349
Beniston M, Jungo P (2002) Shifts in the distributions of pressure, temperature and moisture and changes in the typical weather patterns in the alpine region in response to the behavior of the north atlantic oscillation. Appl Climatol 71(1–2):29–42. https://doi.org/10.1007/s704-002-8206-7
Besselaar EJM, Klein Tank AMG, Buishand, Buishand TA (2013) Trends in European precipitation extremes over 1951–2010. Intl J Climatol 33(12):2682–2689. https://doi.org/10.1002/joc.3619
Böhm R, Auer I, Brunetti M, Maugeri M, Nanni T, Schöner W (2001) Regional temperature variability in the European alps: 1760–1998 from homogenized instrumental time series. Intl J Climatol 21(14):1779–1801. https://doi.org/10.1002/joc.689
Bongiovanni G, Matiu M, Crespi A, Napoli A, Majone B, Zardi D (2024) Eear-clim: a high density observational dataset of daily precipitation and air temperature for the extended European alpine region [data set]. Zenodo. https://doi.org/10.5281/zenodo.14218564
Bongiovanni G, Matiu M, Crespi A, Napoli A, Majone B, Zardi D (2025) Eear-clim: a high-density observational dataset of daily precipitation and air temperature for the extended European alpine region. Earth Syst Sci. Data 17(4):1367–1391. https://doi.org/10.5194/essd-17-1367-2025
Brugnara Y, Brunetti M, Maugeri M, Nanni T, Simolo C (2012) High-resolution analysis of daily precipitation trends in the central alps over the last century. Intl J Climatol 32(9):1406–1422. https://doi.org/10.1002/joc.2363
Brunetti M, Lentini G, Maugeri M, Nanni T, Auer I, Böhm R, Schöner W (2009) Climate variability and change in the greater alpine region over the last two centuries based on multi-variable analysis. Intl J Climatol 29(15):2197–2225. https://doi.org/10.1002/joc.1857
Brunetti M, Maugeri M, Nanni T, Auer I, Böhm R, Schöner W (2006) Precipitation variability and changes in the greater alpine region over the 1800–2003 period. J Geophys Res 111(D11). https://doi.org/10.1029/2005JD006674
Ceppi P, Scherrer SC, Fischer AM, Appenzeller C (2012) Revisiting Swiss temperature trends 1959–2008. Intl J Climatol 32(2):203–213. https://doi.org/10.1002/joc.2260
Cornale P, Senatore R, Battaglini LM, Baratta M (2025) Climate change and livestock welfare in the alps: a comprehensive review. Animals 15(24):3578. https://doi.org/10.3390/ani15243578
Cramer W, Guiot J, Marini K (2020) Medecc (2020) climate and environmental change in the mediterranean basin – current situation and risks for the future. first mediterranean assessment report. Technical report, Union for the Mediterranean, Plan Bleu, UNEP/MAP, Marseille, France. https://doi.org/10.5281/zenodo.4768833
Curci G, Guijarro JA, Antonio LD, Bacco MD, Lena BD, Scorzini AR (2021) Building a local climate reference dataset: application to the abruzzo region (central Italy), 1930–2019. Intl J Climatol 41(8):4414–4436. https://doi.org/10.1002/joc.7081
Dallan E, Borga M, Zaramella M, Marra F (2022) Enhanced summer convection explains observed trends in extreme subdaily precipitation in the eastern Italian alps. Geophys Res Lett 49(5):2021–096727. https://doi.org/10.1029/2021GL096727
de Luis M, Cufar K, Saz M, Longares L, Ceglar A, Bogataj L (2014) Trends in seasonal precipitation and temperature in Slovenia during 1951–2007. Reg Environ Change 14(5):1801–1810. https://doi.org/10.1007/s10113-012-0365-7
Domonkos P (2015) Homogenization of precipitation time series with acmant. Theor Appl Climatol 122(1–2):303–314. https://doi.org/10.1007/s00704-014-1298-5
EEA: regional climate change and adaptation. The alps facing the challenge of changing water resources. EEA report No. 8/2009. 2009
Ferguglia O, Palazzi E, Arnone E (2024) Elevation dependent change in era5 precipitation and its extremes. Clim Dyn 62(8):8137–8153. https://doi.org/10.1007/s00382-024-07328-6
Fioravanti G, Piervitali E, Desiato F (2019) A new homogenized daily data set for temperature variability assessment in Italy. Intl J Climatol 39(15):5635–5654. https://doi.org/10.1002/joc.6177
Folland C, Frich R, Basnett T, Rayner N, Parker D, Horton B (2000) Uncertainties in climate datasets–a challenge for wmo. Bull The World Meteorolog Organ 49(1):59–67
Garcia-Herrera R, Díaz J, Trigo RM, Luterbacher J, Fischer, Fischer EM (2010) E.M.: a review of the European summer heat wave of 2003. Crit Rev Environ Sci Technol 40(4):267–306. https://doi.org/10.1080/10643380802238137

Gerberding K, Schirpke U (2025) Mapping the probability of forest fire hazard across the European alps under climate change scenarios. J Environ Manag 377, 124600 (124600. https://doi.org/10.1016/j.jenvman.2025.124600
Giorgi F (2006) Climate change hot-spots. Geophys Res Lett 33(8). https://doi.org/10.1029/2006GL025734
Giorgi F, Hurrell JW, Marinucci MR, Beniston M (1997) Elevation dependency of the surface climate change signal: a model study. J Clim 10(2):288–296. https://doi.org/10.1175/1520-0442(1997)010%3C0288:EDOTSC%3E2.0.CO;2
Gobiet A, Kotlarski S, Beniston M, Heinrich G, Rajczak J, Stoffel M (2014) 21st century climate change in the European alps—a review. Sci Total Environ 493:1138–1151. https://doi.org/10.1016/j.scitotenv.2013.07.050
Guijarro JA (2023) Climatol: climate tools (series homogenization and derived products). R package version 4.0.0
Gulev SK, Thorne PW, Ahn J, Dentener FJ, Domingues CM, Gerland S, Gong D, Kaufman DS, Nnamchi HC, Quaas J, Rivera JA, Sathyendranath S, Smith SL, Trewin B, Schuckmann K, Vose (2021) Changing state of the climate system. Cambridge University Press, ???, pp 287–422. https://doi.org/10.1017/9781009157896.004
Hamel A, Brunner MI (2024) Trends and drivers of water temperature extremes in mountain rivers. Water Resour Res Res 60(10):2024–037518. https://doi.org/10.1029/2024WR037518
Hock R, Rasul G, Adler C, Caceres B, Gruber S, Hirabayashi Y, Jackson M, Kääb A, Kang S, Kutuzov S, Milner A, Molau U, Morin S, Orlove B, H. S (2019) High mountain areas. In: IPCC special report on the Ocean and cryosphere in a changing climate. Cambridge University Press, Cambridge, United Kingdom and New York, NY, USA, pp 131–202. https://doi.org/10.1017/9781009157964.004
Hunziker S, Brönnimann S, Calle J, Moreno I, Andrade M, Ticona L, Huerta A, Lavado-Casimiro W (2018) Effects of undetected data quality issues on climatological analyses. Clim. Past 14(1):1–20. https://doi.org/10.5194/cp-14-1-2018
Inouye DW (2022) Climate change and phenology. WIREs Clim Change 13(3):764. https://doi.org/10.1002/wcc.764
Koppen W (1936) Das geographische system der klimate. In: Handbuch der Klimatologie, vol 1. Borntraeger, Berlin
Kotlarski S, Gobiet A, Morin S, Olefs M, Rajczak J, Samacoïts R (2023) 21st century alpine climate change. Clim Dyn 60(1–2):65–86. https://doi.org/10.1007/s00382-022-06303-3
Laiti L, Zardi D, de Franceschi M, Rampanelli G (2013) Atmospheric boundary layer structures associated with the ora del garda wind in the alps as revealed from airborne and surface measurements. Atmos Res 132-133:473–489. https://doi.org/10.1016/j.atmosres.2013.07.006
Leys C, Ley C, Klein O, Bernard P, Licata L (2013) Detecting outliers: do not use standard deviation around the mean, use absolute deviation around the median. J Educ Chang Exp Soc Phychol 49(4):764–766. https://doi.org/10.1016/j.jesp.2013.03.013
Luce CH, Abatzoglou JT, Holden ZA (2013) The missing mountain water: slower westerlies decrease orographic enhancement in the pacific northwest USA. Science 342(6164):1360–1364. https://doi.org/10.1126/science.1242335
Menzel A, Yuan Y, Matiu M, Sparks T, Scheifinger H, Gehrig R, Estrella N (2020) Climate change fingerprints in recent European plant phenology. Glob Change Biol 26(4):2599–2612. https://doi.org/10.1111/gcb.15000
Ménégoz M, Valla E, Jourdain NC, Blanchet J, Beaumet J, Wilhelm B, Gallée H, Fettweis X, Morin S, Anquetin S (2020) Contrasting seasonal changes in total and intense precipitation in the European alps from 1903 to 2010. Hydrol Earth Syst Sci 24(11):5355–5377. https://doi.org/10.5194/hess-24-5355-2020
Moberg A, Jones P (2005) Trends in indices for extremes in daily temperature and precipitation in central and western Europe, 1901-99. Int J Climatol 25(9):1149–1171. https://doi.org/10.1002/joc.1163
Monteiro D, Morin S (2023) Multi-decadal analysis of past winter temperature, precipitation and snow cover data in the European alps from reanalyses, climate models and observational datasets. Cryosphere 17(8):3617–3660. https://doi.org/10.5194/tc-17-3617-2023
Mueller B, Seneviratne S (2012) Hot days induced by precipitation deficits at the global scale. Proc Nat Acad Sci USA 109:12398–12403. https://doi.org/10.1073/pnas.1204330109
Napoli A, Crespi A, Ragone F, Maugeri M, Pasquero C (2019) Variability of orographic enhancement of precipitation in the alpine region. Sci Rep 9(1), 13352 (https://doi.org/10.1038/s41598-019-49974-5
Napoli A, Parodi A, Hardenberg J, Pasquero C (2023) Altitudinal dependence of projected changes in occurrence of extreme events in the great alpine region. Intl J Climatol 43(12):5813–5829. https://doi.org/10.1002/joc.8222
Ohmura A (2012) Enhanced temperature variability in high-altitude climate change. Theor Appl Climatol 110(4):499–508. https://doi.org/10.1007/s00704-012-0687-x

Palazzi E, Mortarini L, Terzago S, Hardenberg J (2019) Elevation-dependent warming in global climate model simulations at high spatial resolution. Clim Dyn 52(5–6):2685–2702. https://doi.org/10.1007/s00382-018-4287-z

Panziera L, Gabella M, Germann U, Martius, Martius O (2018) A 12-year radar-based climatology of daily and sub-daily extreme precipitation over the Swiss alps. Intl J Climatol 38(10):3749–3769. https://doi.org/10.1002/joc.5528

Pepin N, Arnone E, Gobiet A, Haslinger K, Kotlarski S, Notarnicola C, Palazzi E, Seibert P, Serafin S, Schöner W, Terzago S, Thornton J, Vuille M, Adler C (2022) Climate changes and their elevational patterns in the mountains of the world. Rev Geophysics 60(1). https://doi.org/10.1029/2020RG000730

Pepin N, Bradley R, Diaz H, Baraer M, Caceres E, Forsythe N, Fowler H, Greenwood G, Hashmi M, Liu X, Miller J, Ning L, Ohmura A, Palazzi E, Rangwala I, Schöner W, Severskiy I, Shahgedanova M, Wang M, Williamson S, Yang D (2015) Elevation-dependent warming in mountain regions of the world. Nat Clim Change 5(5:424–430. https://doi.org/10.1038/nclimate2563

Pepin NC, Lundquist JD (2008) Temperature trends at high elevations: patterns across the globe. Geophys Res Lett 35(14). https://doi.org/10.1029/2008GL034026

Peterson TC (2005) Climate change indices. WMO Bull 54(2):83–86

Philipona R (2013) Greenhouse warming and solar brightening in and around the alps. Intl J Climatol 33(6):1530–1537. https://doi.org/10.1002/joc.3531

Piao S, Liu Q, Chen A, Janssens IA, Fu Y, Dai J, Liu L, Lian X, Shen M, Zhu X (2019) Plant phenology and global climate change: current progresses and challenges. Glob Change Biol 25(6):1922–1940. https://doi.org/10.1111/gcb.14619

Rangwala I, Miller J (2012) Climate change in mountains: a review of elevation-dependent warming and its possible causes. Climatic Change 114(3–4):527–547. https://doi.org/10.1007/s10584-012-0419-3

Rangwala I, Sinsky E, Miller JR (2016) Variability in projected elevation dependent warming in boreal mid-latitude winter in cmip5 climate models and its potential drivers. Clim Dyn 46(7–8):2115–2122. https://doi.org/10.1007/s00382-015-2692-0

Rottler E, Kormann C, Francke T, Bronstert A (2019) Elevation-dependent warming in the Swiss alps 1981–2017: features, forcings and feedbacks. Intl J Climatol 39(5):2556–2568. https://doi.org/10.1002/joc.5970

Rysman J-F, Lemaitre Y, Moreau E (2016) Spatial and temporal variability of rainfall in the alps–mediterranean euroregion. J Appl Meteorol Clim 55(3):655–671. https://doi.org/10.1175/JAMC-D-15-0095.1

Sandrini S, Fuzzi S, Piazzalunga A, Prati P, Bonasoni P, Cavalli F, Bove MC, Calvello M, Cappelletti D, Colombi C, Contini D, de Gennaro G, Di Gilio A, Fermo P, Ferrero L, Gianelle V, Giugliano M, Ielpo P, Lonati G, Marinoni A, Massabò D, Molteni U, Moroni B, Pavese G, Perrino C, Perrone MG, Perrone MR, Putaud J-P, Sargolini T, Vecchi R, Gilardoni S (2014) Spatial and seasonal variability of carbonaceous aerosol across Italy. Atmos Environ 99:587–598. https://doi.org/10.1016/j.atmosenv.2014.10.032

Schlegel RW, Smit (2021). R package version 0.4.6. A.J.: heatwaveR: detect heatwaves and cold-spells. https://CRAN.R-project.org/package=heatwaveR

Schmidli J, Schmutz C, Frei C, Wanner H, Schär C (2002) Mesoscale precipitation variability in the region of the European alps during the 20th century. Intl J Climatol 22(9):1049–1074. https://doi.org/10.1002/joc.769

Schär C, Davies T, Frei C, Wanner H, Widmann M, Wild M, Davies H (1998) Current alpine climate. In: Views from the Alps: regional perspectives on climate change. The MIT Press, ???

Schroeder P, Belis C, Schnelle-Kreis J, Herzig R, Prévôt AS, Raveton M, Kirchner M, Catinon M (2014) Why air quality in the alps remains a matter of concern. The impact of organic pollutants in the alpine area. Environ Sci Pollut Res 21(1):252–267. https://doi.org/10.1007/s11356-013-2058-2

Sen PK (1968) Estimates of the regression coefficient based on Kendall's tau. J Am Stat Assoc 63(324):1379–1389. https://doi.org/10.1080/01621459.1968.10480934

Sippel S, Barnes C, Cadiou C, Fischer E, Kew S, Kretschmer M, Philip S, Shepherd TG, Singh J, Vautard R, Yiou P (2024) Could an extremely cold central European winter such as 1963 happen again despite climate change? Weather Clim. Dynam. 5(3):943–957. https://doi.org/10.5194/wcd-5-943-2024

Sneyers R (1990) On the statistical analysis of series of observations world meteorological organization (wmo). Technical Note 143(192)

Stocker TF, Qin D, Plattner G-K, Tignor MM, Allen SK, Boschung J, Nauels A, Xia Y, Bex V, Midgley PM (2013) Climate change 2013: the physical science basis. Contribution of working group I to the fifth assessment report of the intergovernmental panel on climate change 1535. Cambridge University Press, Cambridge, United Kingdom and New York, NY, USA

Tank AMGK, GP (2003) Trends in indices of daily temperature and precipitation extremes in Europe, 1946–99. J. Clim 16(22):3665–3680. https://doi.org/10.1175/1520-0442(2003)016%3C3665:TIIODT%3E2.0.CO;2

Toreti A, Desiato F (2008) Changes in temperature extremes over Italy in the last 44 years. Intl J Climatol 28(6):733–745. https://doi.org/10.1002/joc.1576

Tudoroiu M, Eccel E, Gioli B, Gianelle D, Schume H, Genesio L, Miglietta F (2016) Negative elevation-dependent warming trend in the eastern alps. Environ Res Lett 11(4), 044021 (044021). https://doi.org/10.1088/1748-9326/11/4/044021

Vose RS, Menne, Menne MJ (2004) A method to determine station density requirements for climate observing networks. J. Clim 17(15):2961–2971. https://doi.org/10.1175/1520-0442(2004)017%3C2961:AMTDSD%3E2.0.CO;2

Wang XL (2008) Accounting for autocorrelation in detecting mean shifts in climate data series using the penalized maximal t or f test. J Appl Meteorol Clim 47(9):2423–2444. https://doi.org/10.1175/2008JAMC1741.1

WMO: calculation of monthly and annual 30-year standard normals. TD-No. 341 (1989)

WMO: Wmo guidelines on the calculation of climate normals. WMO-No.1203 (2017)

Zecchetto S, De Biasio F, Bajo M (2009) Features of scatterometer wind observations in the Adriatic Sea. Cambridge University Press, ???, pp 53–58

Zhang X, Alexander L, Hegerl GC, Jones P, Tank AK, Peterson TC, Trewin B, Zwiers FW (2011) Indices for monitoring changes in extremes based on daily temperature and precipitation data. WIREs Clim Change 2(6):851–870. https://doi.org/10.1002/wcc.147

Zubler E, Scherrer S, Croci-Maspoli M, Liniger M, Appenzeller C (2014) Key climate indices in Switzerland; expected changes in a future climate. Climatic Change 123(2):255–271. https://doi.org/10.1007/s10584-013-1041-8

Authors and Affiliations

Giulio Bongiovanni[1,2] · Anna Napoli[1,3] · Michael Matiu[1] · Alice Crespi[4] · Bruno Majone[1] · Dino Zardi[1]

✉ Giulio Bongiovanni
giulio.bongiovanni@unitn.it

[1] Department of Civil, Environmental and Mechanical Engineering (DICAM), University of Trento, Via Mesiano 77, 38123 Trento, Italy

[2] University School for Advanced Studies Pavia (IUSS), Palazzo del Broletto, Piazza della Vittoria 15, 27100 Pavia, Italy

[3] Center for Agriculture Food Environment (C3A), University of Trento, Via Edmund Mach 1, 38098 San Michele all'Adige, Italy

[4] Center for Climate Change and Transformation (CCT), Eurac Research, Viale Druso 1, 39100 Bozen, Italy